Journal of Solid State Chemistry 288 (2020) 121421

Contents lists available at ScienceDirect

Journal of Solid State Chemistry

journal homepage: www.elsevier.com/locate/jssc

Metal-organic framework-derived sulfur and nitrogen dual-doped bimetallic carbon nanotubes as electrocatalysts for oxygen evolution reaction

Hongxu Chen [1], Yuwen Li [1], Huajian Liu, Qinghong Ji, Lijia Zou, Junkuo Gao *

The Key Laboratory of Advanced Textile Materials and Manufacturing Technology of Ministry of Education, College of Materials and Textiles, Zhejiang Sci-Tech University, Hangzhou, 310018, China

ARTICLE INFO

Keywords:
Metal-organic frameworks
Dual-doping
Bimetallic
Nanotube
Oxygen evolution reaction
Electrocatalysis

ABSTRACT

Metal-organic frameworks (MOFs) are attracting more and more attention in the field of electrocatalysis because of their porosity, ease of adjustment and functionalization. Herein, we report the preparation of sulfur-nitrogen dual-doped Co–Fe bimetallic carbon nanotubes (CoFe@SNCN) using MOFs as precursors. The optimized CoFe@SNCN achieves a current density of 10 mA cm^{-2} at a low overpotential of 306.4 mV with a very small Tafel slope of 76.0 mV dec^{-1} in 1 M KOH, which is 64 mV smaller than that of Co@SNCN (370.4 mV) and 48 mV smaller than that of Fe@SNCN (354.4 mV). Moreover, the catalytic performance remains almost unchanged after 12 h. The excellent electrocatalytic performance can be attributed to the synergies between the bimetals and heteroatoms doping, which can greatly improve the electrical conductivity between the metals, promote the transfer of electrons and the exchange of substances, thereby greatly reducing the reaction kinetics and enhancing OER properties. This work may provide a very good solution for the research of a new type of highly efficient stable electrocatalytic oxygen evolution catalyst.

1. Introduction

Increasingly serious ecological and environmental problems and expanding energy demand in various industries have greatly promoted more research on the development of renewable energy [1]. Due to its excellent energy density, high energy conversion efficiency and pollution-free characteristics, hydrogen energy is considered to be one of the best energy sources in the future [2]. Overall water splitting is one of the most effective and sustainable methods for the production of hydrogen, which helps to meet the above-mentioned increasingly severe energy needs and also promote the development of human survival and civilization [3,4]. The half reaction of water decomposition, oxygen evolution reaction (OER), plays a vital role in determining the overall performance of the reaction [5]. A series of studies have shown that an excellent OER electrocatalyst must have characteristics including low overpotential, small Tafel slope, and good stability as the reaction proceeds [6]. Precious metal oxide catalysts such as IrO_2 and RuO_2 in the anode are currently the best catalysts for OER [7]. But unfortunately, the disadvantages of their high price and scarce resources have greatly limited their wide application [8]. Therefore, the development of cheap and efficient electrocatalysts is extremely necessary [9].

Transition metals exhibit very good catalytic development prospects due to their special extranuclear electronic structures, especially cobalt, iron and nickel have been widely reported [10–12]. It is well known that the interaction between various compositions in a multi-metal structure can produce additional synergistic effects and lead to better electronic properties. Fe–Co-based OER catalysts have attracted widespread attention attribute to their excellent OER activity and stability in alkaline solutions [13]. Fe tends to act as the main active site, while Co provides the backbone for electron framework [14,15]. Forming a heteroatom doping structure is also widely considered as a new strategy to design new electrocatalysts. Heteroatoms doping like nitrogen and sulfur has been proved to induce higher spin density and modulate the electron densities and structures of catalytic active sites, thereby further improving the electrocatalytic activities [16]. For example, Yu et al. used ZnCo-ZIFs to synthesize N, S-codoped carbon nanotube and nanopolyhedra and it was highly efficient for both HER and OER [17].

Except for the composition, the structural design of the catalyst is also important. Recently, metal–organic frameworks (MOFs) with well-defined chemical structures and morphologies have emerged as an ideal platform and precursors for the synthesis of new nanocarbon composites [18,19]. MOFs are network-like frameworks formed by self-assembly of

---

* Corresponding author.
E-mail address: jkgao@zstu.edu.cn (J. Gao).

[1] These authors contributed equally to this paper.

https://doi.org/10.1016/j.jssc.2020.121421
Received 16 April 2020; Received in revised form 25 April 2020; Accepted 28 April 2020

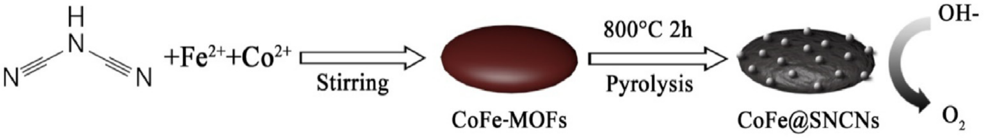

Scheme 1. Schematic illustariong of the preparation process of CoFe@SNCNs.

metal ions or clusters and organic ligands [20]. And they have been used in various fields, like supercapacitor (SC) [21–24], photocatalytic dye degradation [25], adsorption of pharmaceutical intermediates in wastewater [26], refining and purification of fuel [27,28] and catalysis [29]. MOFs own high porosities and the uniformity of their pore and channel sizes accounts for much of their catalytic selectivity [30,31], which is useful to improve the electrocatalytic performance of carbon materials. The well-organized framework can be converted to carbon with uniform heteroatoms decoration, and the long-range ordering and high porosity of MOFs can be partially preserved to afford high surface area of resultant porous carbons via facile pyrolysis [32]. For example, You et al. fabricated porous CoP_x nanoparticles embedded in N-doped carbon matrices were obtained by direct carbonization and phosphidation of a Co-based MOF (zeolitic imidazolate framework-67, ZIF-67), and it can be used as a catalyst for OER [33,34]. In recent years, some new synthetic methods, such as surfactant-thermal method, ionothermal method, deep eutectic solvent method and mechanochemistry method, have been used in the preparation of crystalline inorganic-organic hybrid materials [35–40]. The rapid development of MOF synthesis methods has led to the production of a large number of new MOF materials [41]. At the meanwhile, a series of studies have shown that nanostructures demonstrate great potentials in catalysis and their compositions may cause some interferences in the reactivity. Furthermore, the use of bimetallic nano-structures as nanocatalysts is more conducive to accelerating reactions than single metal catalysts [42–44]. In particular, bimetallic nanocarbon materials prepared with MOFs as templates have very good electrocatalytic application prospects [45].

Herein, we report a sulfur-nitrogen dual-doped Co–Fe bimetallic electrocatalyst (CoFe@SNCN) by using MOFs as templates to introduce a sulfurand nitrogen-doped carbon nanotubes. Compared with single metallic Co@SNCN and Fe@SNCS, the electrocatalytic oxygen evolution performance of CoFe@SNCN has been significantly improved, which is due to the synergies between the bimetals and heteroatoms doping. When the current density is 10 mA cm^{-2}, the optimized CoFe@SNCN reaches 306.4 mV, and the Tafel slope is 76.0 mV dec^{-1}, together with an exceptional long-term stability in the oxygen release reaction.

2. Results and discussions

Based on the experimental preparation of Co@SNCN, a bimetallic CoFe@SNCN catalyst was synthesized by doping with iron (as shown in Scheme 1). Briefly introduced as follows, at room temperature (25 °C), two metal salts Fe $(ClO_4)_2 \cdot xH_2O$ and $Co(NO_3)_2{\cdot}6H_2O$, are dissolved in a Dimethyl Sulfoxide (DMSO) solution. The DMSO solution can introduce sulfur into the MOFs. Subsequent two metals Coordination of ions with sodium dicyandiamide, after 4 h of stirring reaction, CoFe MOFs were finally obtained. The obtained sample was calcined in a nitrogen atmosphere at 800 °C for 2 h, and then subjected to an acid leaching treatment to remove other impurities. Finally, sulfur-nitrogen dual-doped Co–Fe bimetallic carbon nanotubes (CoFe@SNCNs) using MOFs as templates were formed.

Scanning electron microscope (SEM) was used to study the subtle morphology of CoFe@SNCN. Fig. 2a and b shows SEM images of CoFe-MOF in low magnification and high magnification, respectively. CoFe-MOF has an irregular appearance and is made of irregular flaky objects. Whereas, after the pyrolysis process (as shown in Fig. 1c and d), the morphology of CoFe@SNCN tends to be regular, resemble a group of blood cells with a size of 1.2 μm in the horizontal direction and 1 μm in the longitudinal direction. After observing carefully, it is composed of several carbon nanotubes. At the meanwhile, a porous surface is formed, which helps increase the exposed area and the rapid diffusion of the electrolyte [46]. It is particularly noteworthy that it can be clearly seen from Fig. 1d that some carbon nanotubes are formed due to Fe and Co, which easily form carbon nanotubes [47]. As shown in the darker area in Fig. 1e, the nanoparticles are embedded in the ends of the nanotubes. This structure will promote efficient electron transfer and enhance catalyst stability during electrocatalysis. Therefore, CoFe@SNCN shows an excellent electrocatalytic performance in OER.

The X-ray diffraction (XRD) pattern of CoFe-MOFs is showed in Figure S1. The XRD data revealed that the CoFe-MOF and Co-MOF diffraction peaks were consistent, which confirmed the successful synthesis of the precursor templates. The peaks in the CoFe-MOF XRD spectrum are weaker. This may suggest a small size feature and possibly a low

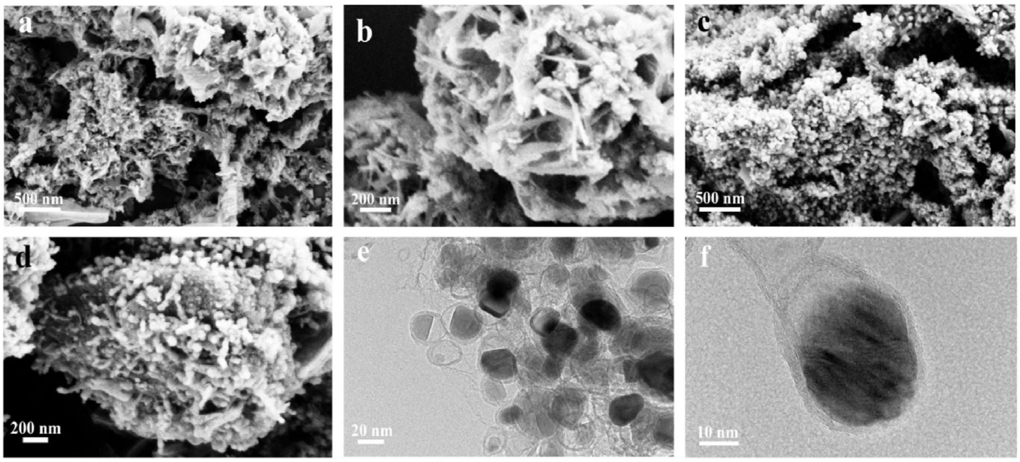

Fig. 1. SEM images of CoFe-MOF in a) low magnification and b) high magnification. c,d) SEM images and d,e) TEM images of CoFe@SNCN.

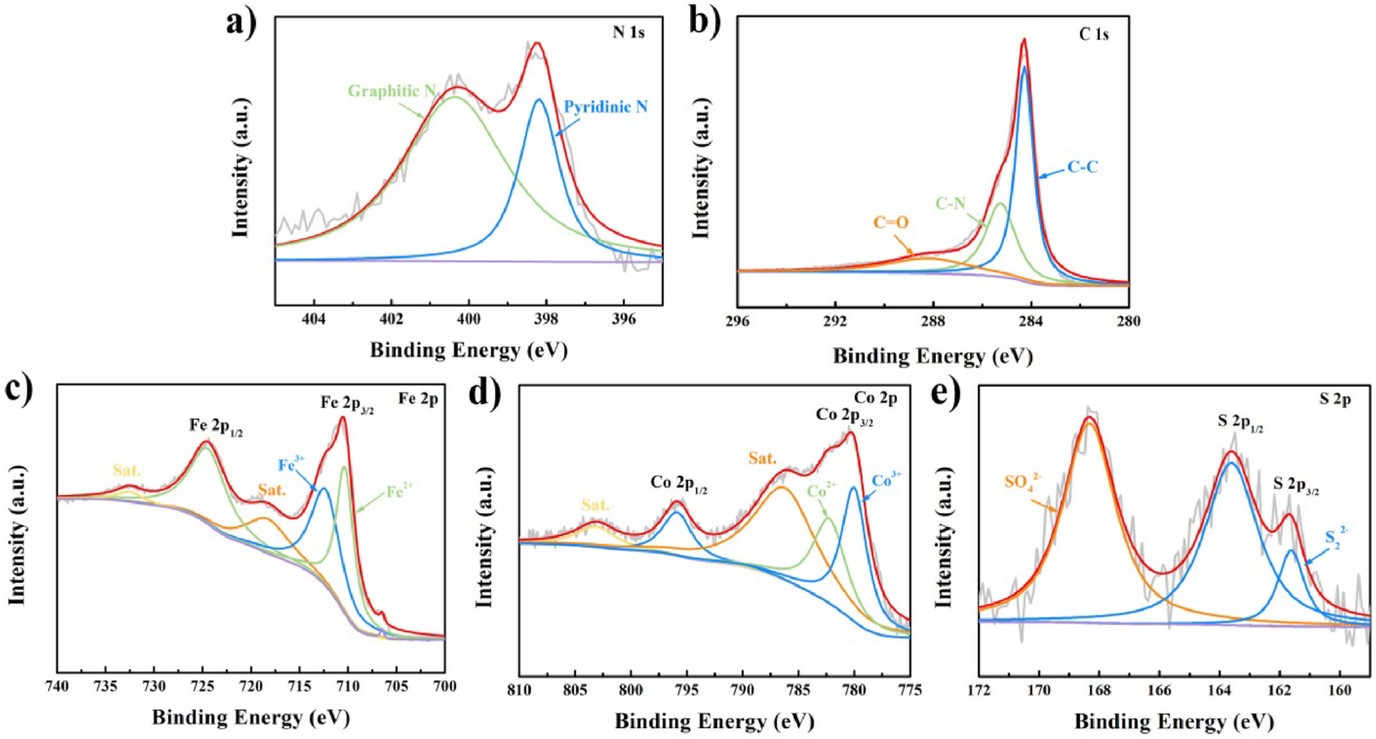

Fig. 2. High resolution a) N 1s, b) C 1s, c) Fe 2p, d) Co 2p and e) S 2p XPS spectra of CoFe@SNCN.

crystallization property of the as-formed products. X-ray photoelectron spectroscopy (XPS) was introduced to further investigate the surface chemistry of CoFe@SNCN materials. As revealed by the XPS survey spectrum, CoFe@SNCN contains 75.75, 1.37, 11.94, and 4.22 at% C, S, Fe, and Co, respectively (supported in Figure S4). N species was confirmed to be 6.52 at%. The bonding state of N in CoFe@SNCN was analyzed by a high-resolution N 1s spectrum. The spectrum was deconvoluted into two peaks (Fig. 2a), pyridinic N (398.2 eV) and graphitic N (400.4 eV) [48,49]. What is worth noting that the plentiful pyridinic N can coordinate with metal atoms through the metal-N-C structure to optimize the local electronic structure and facilitate the electrochemical process [50]. Furthermore, the C 1s spectrum confirmed the presence of C–C (284.3eV), C–N (285.3eV), and C=O (288.2eV) in CoFe@SNCN (Fig. 2b) [50]. In Fig. 2c, the Fe 2p spectra of CoFe@SNCN show two main peaks of Fe $2p_{3/2}$ and Fe $2p_{1/2}$ at 710.5 eV and 724.5 eV, respectively, and two satellites at 718.5 eV and 732.6 eV. After deconvolution, the peaks located at 710.4 and 724.7 eV were attributed to Fe^{2+}, and the peak centered at 712.5 eV was assigned to Fe^{3+} [51]. The XPS spectrum of Co 2p shows the existence of Co^{2+} and Co^{3+}. The $2p_{1/2}$ peak can be deconvoluted to Co^{3+} at 796.0 eV and the fitting peaks at 782.3 and 780.0 eV represent the Co^{2+} $2p_{3/2}$ and Co^{3+} $2p_{3/2}$, together with two satellite peaks at 786.5 eV and 803.3 eV, respectively (Fig. 2d). Then, the S $2p_{3/2}$ and S $2p_{1/2}$ peaks of S^{2-} are concentrated at 161.7 eV and 163.6 eV (Fig. 2e).

Brunauer-Emmett-Teller (BET) facilitates measurement of specific surface area and pore structure. As shown in Fig. 3, it can be observed that the typical type IV adsorption isotherm has an obvious hysteresis loop, which indicates the existence of micro/mesopores in CoFe@SNCN. The specific surface area of CoFe@SNCN was determined to be 192.7 m^2 g^{-1}, and the pore diameter was 2.64 nm. The larger specific surface area is beneficial to expose more active sites and improve the electrocatalytic performance.

The electrocatalytic OER performance of Co@SNCN, Fe@SNCN and CoFe@SNCN on nickel foam electrodes was evaluated by a standard three-electrode system in 1 M KOH at a scan rate of 5 mV s^{-1}. Fig. 4a shows the OER polarization curves of Co@SNCN, Fe@SNCN and CoFe@SNCN with a reversible hydrogen electrode (RHE). All polarization curves were performed without iR compensation. In Fig. 4a, the Co@SNCN shows the worst catalytic performance, with an overpotential of 370.4 mV at 10 mA cm^{-2}. When iron was added, the overpotential at 10 mA cm^{-2} decreased to 306.4 mV. At the same time, the overpotential of the single-metal Fe@SNCN was measured to be 354.4 mV, and the performance was also worse than that of the bimetallic electrocatalyst. CoFe@SNCN shows an ultra-low overpotential which is superior to most OER catalysts (Table S1). On the one hand, for cobalt electrocatalyst, it is noteworthy that the catalytic active sites locate at cobalt sites. And catalytic efficiency of cobalt-based catalyst is highly influenced by the microchemical environmental of cobalt sites. The activity of cobalt centers would be enhanced by

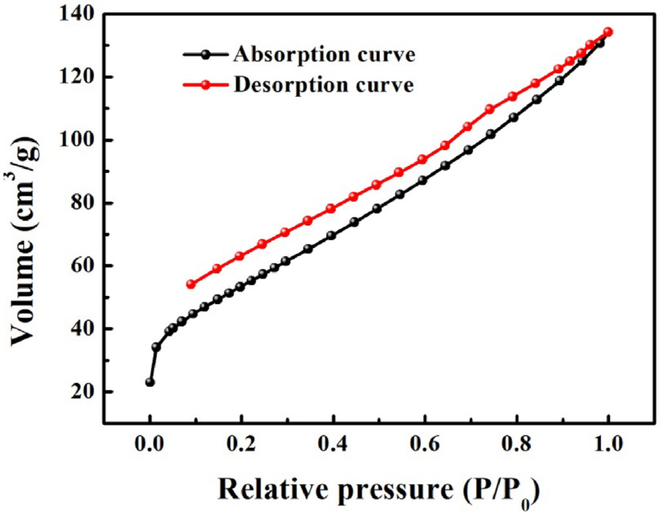

Fig. 3. The nitrogen sorption isotherm of CoFe@SNCN.

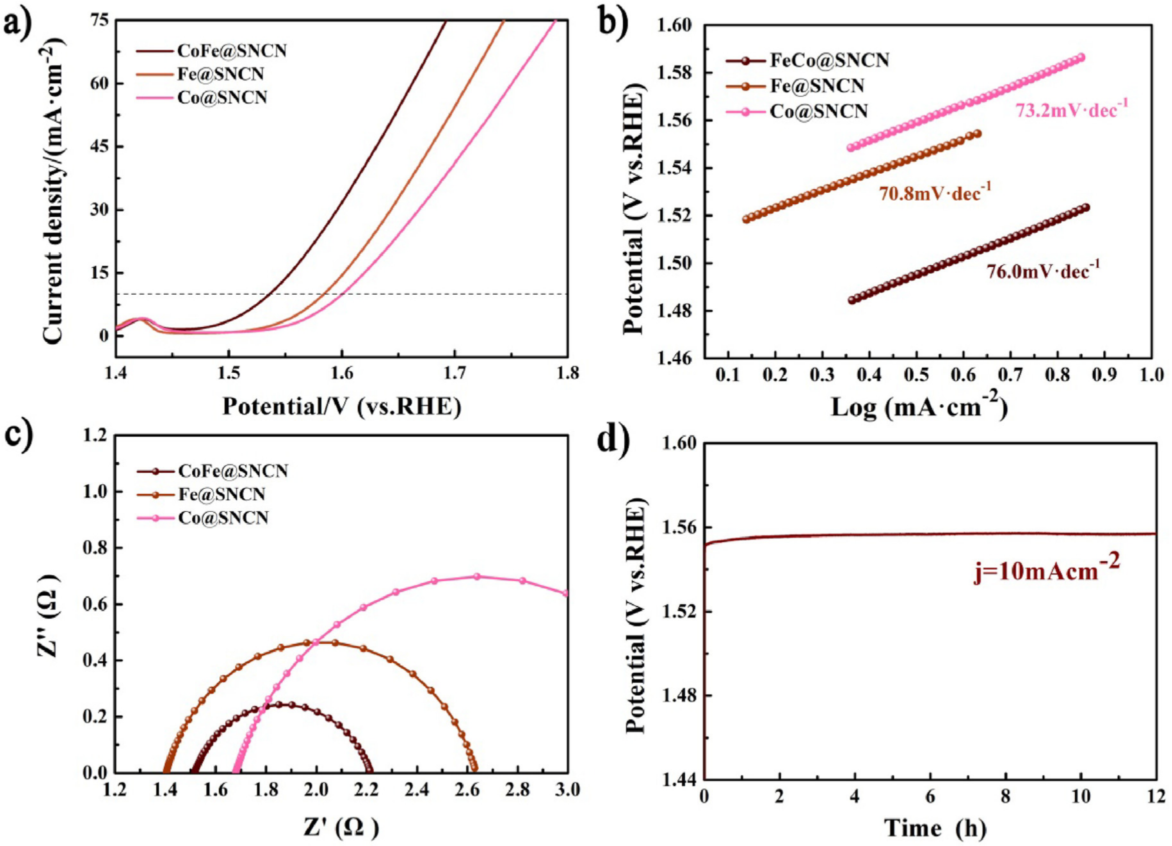

Fig. 4. (a) The OER polarization curves of CoFe@SNCN in a 1 M KOH solution at a scan rate of 5 mV s^{-1}. (b) Tafel slope plots of CoFe@SNCN. (c) Electrochemical impedance spectra of CoFe@SNCN. (d) Chronopotentiometric test (V-t curve) of CoFe@SNCN for 12 h.

introducing doping ions, supports, or another functional composition [52, 53]. The composite catalysts often show enhanced catalytic performances due to the synergetic chemical coupling effects between them [5]. On the other hand, it has been reported that doping foreign metal atoms with similar electronic configuration into the original lattice can significantly optimize the electronic structure of the active site, thereby significantly improving the electrocatalytic activity of the transition metal-based electrocatalyst [8]. Furthermore, the Tafel slope is a direct method to evaluate the effect of the speed-limiting step on the electrocatalytic reaction process. The electrocatalytic kinetics of the three electrocatalysts were further evaluated by the Tafel slope. In line with the polarization curve, the Tafel slope of CoFe@SNCN, Co@SNCN and Fe@SNCN is 76.0 mV dec^{-1}, 73.2 mV dec^{-1} and 70.8 mV dec^{-1} respectively. What's more, electrochemical impedance spectroscopy (EIS) was performed to evaluate the interfacial electron/proton transfer activity of the electrocatalyst. This technique can detect relaxation processes in the large frequency domain based on the interrupt method [9]. The adsorption of reactive intermediates (general intermediates in OER) on the electrode surface is indicated by a low-frequency semicircle, and the high-frequency semicircle corresponds to the charge transfer process. As shown in Fig. 4c, the semicircle radius generated by CoFe@SNCN in the high-frequency region is smaller than Co@SNCN and Fe@SNCN, which explains that CoFe@SNCN has a higher charge transport efficiency than Co@SNCN and Fe@SNCN during the electrochemical OER process. This phenomenon illustrates that the combination of bimetals can reduce the charge transfer resistance and improve the electrocatalytic performance. Additionally, long-term durability is considered a key indicator for practical applications. To further test the durability of CoFe@SNCN, Fig. 4d shows the chronopotential curve of CoFe@SNCN tested at a constant current density (10 mA cm^{-2}). After 12 h of continuous operation, the voltage remains good, which indicates its excellent stability.

3. Conclusion

In this study, we report a sulfur-nitrogen dual-doped Co–Fe bimetallic carbon nanotubes electrocatalyst (CoFe@SNCN) prepared using MOFs as templates, which has outstanding and stable OER activity. CoFe@SNCN has an overpotential of 306.4 mV at 10 mA cm^{-2} and a Tafel slope of 76.0 mV dec^{-1}, which is better than both single metallic Co@SNCN and Fe@SNCN. The experimental results prove that the catalyst obtains an optimized bimetallic electronic structure after the introduction of iron, thereby improving the conductivity and electron transfer ability. It has been shown that the synergistic effect of bimetals and S, N-doping can improve the electrocatalytic performance. We will continue to develop and prepare electrocatalysts with better performance using MOFs as templates and transition metals as raw materials.

Supporting information

The Experimental Section, XRD, SEM, BET, and XPS spectra of the samples.

Declaration of competing interest

The authors declare that they have no known competing financial interests or personal relationships that could have appeared to influence the work reported in this paper.

CRediT authorship contribution statement

Hongxu Chen: Writing - original draft. **Yuwen Li:** Writing - original draft. **Qinghong Ji:** Formal analysis. **Lijia Zou:** Formal analysis. **Junkuo Gao:** Supervision.

Acknowledgments

This work was supported by the Zhejiang Provincial Natural Science Foundation of China (LY20E020001), National Natural Science Foundation of China (51602301and 51672251). J.G. acknowledges the Fundamental Research Funds of Zhejiang Sci-Tech University (2019Q007).

Appendix A. Supplementary data

Supplementary data to this article can be found online at https://doi.org/10.1016/j.jssc.2020.121421.

References

[1] Z. Zhao, M. Li, L. Zhang, L. Dai, Z. Xia, Design principles for heteroatom-doped carbon nanomaterials as highly efficient catalysts for fuel cells and metal-air batteries, Adv. Mater. 27 (2015) 6834–6840.

[2] (a) M. Lu, Y. Li, P. He, J. Cong, D. Chen, J. Wang, Y. Wu, H. Xu, J. Gao, J. Yao, Bimetallic metal-organic framework nanosheets as efficient electrocatalysts for oxygen evolution reaction, J. Solid State Chem. 272 (2019) 32–37;
(b) L. Wang, H. Xu, J. Gao, J. Yao, Q. Zhang, Recent progress in metal-organic frameworks-based hydrogels and aerogels and their applications, Coord. Chem. Rev. 398 (2019) 213016;
(c) C. Li, H. Xu, J. Gao, W. Du, L. Shangguan, X. Zhang, R.-B. Lin, H. Wu, W. Zhou, X. Liu, J. Yao, B. Chen, Tunable titanium metal-organic frameworks with infinite 1D Ti-O rods for efficient visible-light-driven photocatalytic H_2 evolution, J. Mater. Chem. A 7 (2019) 11928–11933;
(d) J. Gao, X. Qian, R. Lin, R. Krishna, H. Wu, W. Zhou, B. Chen, Mixed metal-organic framework with multiple binding sites for efficient C_2H_2/CO_2 separation, Angew. Chem. Int. Ed. 59 (2020) 4396–4400.

[3] J. Zhao, X. Zhang, M. Liu, Y.-Z. Jiang, M. Wang, Z.-Y. Li, Z. Zhou, Metal–organic-framework-derived porous 3D heterogeneous $NiFe_x/NiFe_2O_4$@NC nanoflowers as highly stable and efficient electrocatalysts for the oxygen-evolution reaction, J. Mater. Chem. A 7 (2019) 21338–21348.

[4] D. Pletcher, X. Li, Prospects for alkaline zero gap water electrolysers for hydrogen production, Int. J. Hydrogen Energy 36 (2011) 15089–15104.

[5] J. Yang, G. Zhu, Y. Liu, J. Xia, Z. Ji, X. Shen, S. Wu, Fe_3O_4-Decorated Co_9S_8 nanoparticles in situ grown on reduced graphene oxide: a new and efficient electrocatalyst for oxygen evolution reaction, Adv. Funct. Mater. 26 (2016) 4712–4721.

[6] Y. Fu, W. Wang, J. Wang, X. Li, R. Shi, O. Peng, B.N. Chandrashekar, K. Liu, A. Amini, C. Cheng, MOFs-derived ZnCo–Fe core–shell nanocages with remarkable oxygen evolution reaction performance, J. Mater. Chem. A 7 (2019) 17299–17305.

[7] H. Kim, J. Kim, S.H. Ahn, Monitoring oxygen-vacancy ratio in NiFe-based electrocatalysts during oxygen evolution reaction in alkaline electrolyte, J. Ind. Eng. Chem. 72 (2019) 273–280.

[8] (a) Y. Li, T. Zhao, M. Lu, Y. Wu, Y. Xie, H. Xu, J. Gao, J. Yao, G. Qian, Q. Zhang, Enhancing oxygen evolution reaction through modulating electronic structure of trimetallic electrocatalysts derived from metal-organic frameworks, Small 15 (2019) 1901940;
(b) Y. Li, M. Lu, Y. Wu, H. Xu, J. Gao, J. Yao, Trimetallic metal-organic framework derived carbon-based nanoflower electrocatalysts for efficient overall water splitting, Adv. Mater. Interfaces 6 (2019) 1900290;
(c) Y. Li, M. Lu, P. He, Y. Wu, J. Wang, D. Chen, H. Xu, J. Gao, J. Yao, Bimetallic metal-organic framework-derived nanosheet-assembled nanoflower electrocatalysts for efficient oxygen evolution reaction, Chem. Asian J. 14 (9) (2019) 1590–1594.

[9] T. Zhao, J. Gao, J. Wu, P. He, Y. Li, J. Yao, Highly active cobalt/tungsten carbide@N-doped porous carbon nanomaterials derived from metal-organic frameworks as bifunctional catalysts for overall water splitting, Energy Technol. 7 (2019) 1800969.

[10] D. Li, J. Shi, C. Li, Transition-metal-based electrocatalysts as cocatalysts for photoelectrochemical water splitting: a mini review, Small 14 (2018) 1704179.

[11] G. Liu, R. Yao, Y. Zhao, M. Wang, N. Li, Y. Li, X. Bo, J. Li, C. Zhao, Encapsulation of Ni/Fe_3O_4 heterostructures inside onion-like N-doped carbon nanorods enables synergistic electrocatalysis for water oxidation, Nanoscale 10 (2018) 3997–4003.

[12] R. Xu, R. Wu, Y. Shi, J. Zhang, B. Zhang, Ni_3Se_2 nanoforest/Ni foam as a hydrophilic, metallic, and self-supported bifunctional electrocatalyst for both H_2 and O2 generations, Nano Energy 24 (2016) 103–110.

[13] X. Zhang, X. Zhang, H. Xu, Z. Wu, H. Wang, Y. Liang, Iron-doped cobalt monophosphide nanosheet/carbon nanotube hybrids as active and stable electrocatalysts for water splitting, Adv. Funct. Mater. 27 (2017) 1606635.

[14] M. Xiong, D.G. Ivey, Composition effects of electrodeposited Co-Fe as electrocatalysts for the oxygen evolution reaction, Electrochim. Acta 260 (2018) 872–881.

[15] M.S. Burke, M.G. Kast, L. Trotochaud, A.M. Smith, S.W. Boettcher, Cobalt-iron (oxy) hydroxide oxygen evolution electrocatalysts: the role of structure and composition on activity, stability, and mechanism, J. Am. Chem. Soc. 137 (2015) 3638–3648.

[16] C. Tang, Q. Zhang, Nanocarbon for oxygen reduction electrocatalysis: dopants, edges, and defects, Adv. Mater. 29 (2017) 1604103.

[17] Z. Yu, Y. Bai, S. Zhang, Y. Liu, N. Zhang, K. Sun, Metal–organic framework-derived $Zn_{0.975}Co_{0.025}S/CoS_2$ embedded in N,S-codoped carbon nanotube/nanopolyhedra as an efficient electrocatalyst for overall water splitting, J. Mater. Chem. A 6 (2018) 10441–10446.

[18] B.Y. Xia, Y. Yan, N. Li, H.B. Wu, X.W. Lou, X. Wang, A metal–organic framework-derived bifunctional oxygen electrocatalyst, Nat. Energy 1 (2016) 15006.

[19] Y. Wang, W. Wu, Y. Rao, Z. Li, N. Tsubaki, M. Wu, Cation modulating electrocatalyst derived from bimetallic metal–organic frameworks for overall water splitting, J. Mater. Chem. A 5 (2017) 6170–6177.

[20] Z. Liang, C. Qu, D. Xia, R. Zou, Q. Xu, Atomically dispersed metal sites in MOF-based materials for electrocatalytic and photocatalytic energy conversion, Angew. Chem. Int. Ed. 57 (2018) 9604–9633.

[21] K. Wang, J. Xu, A. Lu, Y. Shi, Z. Lin, Coordination polymer template synthesis of hierarchical $MnCo_2O_{4.5}$ and $MnNi_6O_8$ nanoparticles for electrochemical capacitors electrode, Solid State Sci. 58 (2016) 70–79.

[22] K. Wang, X. Wang, D. Zhang, H. Wang, Z. Wang, M. Zhao, R. Xi, H. Wu, M. Zheng, Interpenetrated nano-MOFs for ultrahigh-performance supercapacitors and excellent dye adsorption performance, CrystEngComm 20 (2018) 6940–6949.

[23] K. Wang, B. Lv, Z. Wang, H. Wu, J. Xu, Q. Zhang, Two-fold interpenetrated Mn-based metal-organic frameworks (MOFs) as battery-type electrode materials for charge storage, Dalton Trans. 49 (2020) 411–417.

[24] K. Wang, Z. Wang, S. Wang, Y. Chu, R. Xi, X. Zhang, H. Wu, Layered Cu^I -MOFs containing $[Mo_8O_{26}]^{4-}$ clusters as supercapacitor electrode materials, Chem. Eng. J. 367 (2019) 239–248.

[25] H.E. Emam, H.B. Ahmed, E. Gomaa, M.H. Helal, R.M. Abdelhameed, Doping of silver vanadate and silver tungstate nanoparticles for enhancement the photocatalytic activity of MIL-125-NH_2 in dye degradation, J. Photochem. Photobiol. Chem. 383 (2019) 111986.

[26] R.M. Abdelhameed, H.E. Emam, Design of ZIF(Co&Zn)@wool composite for efficient removal of pharmaceutical intermediate from wastewater, J. Colloid Interface Sci. 552 (2019) 494–505.

[27] H.E. Emam, A.E. Abdelhamid, R.M. Abdelhameed, Refining of liquid fuel from N-Containing compounds via using designed Polysulfone@Metal organic framework composite film, J. Clean. Prod. 218 (2019) 347–356.

[28] R.M. Abdelhameed, H.R. el-deib, F.M.S.E. El-Dars, H.B. Ahmed, H.E. Emam, Applicable strategy for removing liquid fuel nitrogenated contaminants using MIL-53-NH_2@Natural fabric composites, Ind. Eng. Chem. Res. 57 (2018) 15054–15065.

[29] L. Zhu, X.Q. Liu, H.L. Jiang, L.B. Sun, Metal-organic frameworks for heterogeneous basic catalysis, Chem. Rev. 117 (2017) 8129–8176.

[30] J. Lee, O.K. Farha, J. Roberts, K.A. Scheidt, S.T. Nguyen, J.T. Hupp, Metal-organic framework materials as catalysts, Chem. Soc. Rev. 38 (2009) 1450–1459.

[31] K.-B. Wang, Q. Xun, Q. Zhang, Recent progress in metal-organic frameworks as active materials for supercapacitors, Energy Chem 2 (2020) 100025.

[32] Y.Z. Chen, C. Wang, Z.Y. Wu, Y. Xiong, Q. Xu, S.H. Yu, H.L. Jiang, From bimetallic metal-organic framework to porous carbon: high surface area and multicomponent active dopants for excellent electrocatalysis, Adv. Mater. 27 (2015) 5010–5016.

[33] B. You, N. Jiang, M. Sheng, S. Gul, J. Yano, Y. Sun, High-performance overall water splitting electrocatalysts derived from cobalt-based metal–organic frameworks, Chem. Mater. 27 (2015) 7636–7642.

[34] C. Sun, Q. Dong, J. Yang, Z. Dai, J. Lin, P. Chen, W. Huang, X. Dong, Metal–organic framework derived $CoSe_2$ nanoparticles anchored on carbon fibers as bifunctional electrocatalysts for efficient overall water splitting, Nano Res 9 (2016) 2234–2243.

[35] J.-N. Zhu, X.-Q. Zhu, F.-F. Cheng, P. Li, F. Wang, Y.-W. Xiao, W.-W. Xiong, Preparing copper doped carbon nitride from melamine templated crystalline copper chloride for Fenton-like catalysis, Appl. Catal. B Environ. 256 (2019) 117830.

[36] M.Y. Zhao, J.N. Zhu, P. Li, W. Li, T. Cai, F.F. Cheng, W.W. Xiong, Structural variation of transition metal-organic frameworks using deep eutectic solvents with different hydrogen bond donors, Dalton Trans. 48 (2019) 10199–10209.

[37] D.-D. Yang, W. Li, W.-W. Xiong, J.-R. Li, X.-Y. Huang, Ionothermal synthesis of discrete supertetrahedral Tn (n=4, 5) clusters with tunable components, band gaps, and fluorescence properties, Dalton Trans. 47 (2018) 5977–5984.

[38] W.W. Xiong, E.U. Athresh, Y.T. Ng, J. Ding, T. Wu, Q. Zhang, Growing crystalline chalcogenidoarsenates in surfactants: from zero-dimensional cluster to three-dimensional framework, J. Am. Chem. Soc. 135 (2013) 1256–1259.

[39] W.-W. Xiong, J. Miao, K. Ye, Y. Wang, B. Liu, Q. Zhang, Threading chalcogenide layers with polymer chains, Angew. Chem. Int. Ed. 54 (2015) 546–550.

[40] W.-W. Xiong, Q. Zhang, Surfactants as promising media for the preparation of crystalline inorganic materials, Angew. Chem. Int. Ed. 54 (2015) 11616–11623.

[41] P. Li, F. Cheng, W. Xiong, Q. Zhang, New synthetic strategies to prepare metal-organic frameworks, Inorg. Chem. Front. 5 (2018) 2693–2708.

[42] H.E. Emam, M.M. Mikhail, S. El-Sherbiny, K.S. Nagy, H.B. Ahmed, Metal-dependent nano-catalysis in reduction of aromatic pollutants, Environ. Sci. Pollut. Res. Int. 27 (2020) 6459–6475.

[43] H.E. Emam, M.A. Attia, F.M.S.E. El-Dars, H.B. Ahmed, Emerging use of homogenic and heterogenic nano-colloids synthesized via size-controllable technique in catalytic potency, J. Polym. Environ. 28 (2019) 553–565.

[44] H.B. Ahmed, H.E. Emam, Synergistic catalysis of monometallic (Ag, Au, Pd) and bimetallic (Ag-Au, Au-Pd) versus trimetallic (Ag-Au-Pd) nanostructures effloresced via analogical techniques, J. Mol. Liq. 287 (2019) 110975.

[45] J. Zhou, Y. Dou, A. Zhou, R.-M. Guo, M.-J. Zhao, J.-R. Li, MOF template-directed fabrication of hierarchically structured electrocatalysts for efficient oxygen evolution reaction, Adv. Energy Mater. 7 (2017) 1602643.

[46] P. He, Y. Wu, H. Chen, Z. Zhu, H. Liu, J. Gao, H. Xu, Hierarchical bimetal embedded in carbon nanoflower electrocatalysts derived from metal-organic frameworks for efficient oxygen evolution reaction, J. Alloys Compd. 813 (2020) 152192.

[47] M. Lu, X. Yang, Y. Li, Z. Zhu, Y. Wu, H. Xu, J. Gao, J. Yao, Modulating the electronic structure of porous nanocubes derived from trimetallic metal-organic frameworks

to boost oxygen evolution reaction performance, Chem. Asian J. 14 (2019) 3357–3362.

[48] (a) K. Qiu, G. Chai, C. Jiang, M. Ling, J. Tang, Z. Guo, Highly efficient oxygen reduction catalysts by rational synthesis of nanoconfined maghemite in a nitrogen-doped graphene framework, ACS Catal. 6 (2016) 3558–3568;
(b) S.B. Maddinedi, J. Sonamuthu, S.S. Yildiz, G. Han, Y. Cai, J. Gao, Q. Ni, J. Yao, Silk sericin induced fabrication of reduced graphene oxide and its in-vitro cytotoxicity, photothermal evaluation, J. Photochem. Photobiol., B 186 (2018) 189–196;
(c) J. Gao, Y. Cui, J. Yu, W. Lin, Z. Wang, G. Qian, Enhancement of nonlinear optical activity in new six-branched dendritic dipolar chromophore, J. Mater. Chem. 21 (2011) 3197–3203.

[49] W. Niu, L. Li, X. Liu, N. Wang, J. Liu, W. Zhou, Z. Tang, S. Chen, Mesoporous N-doped carbons prepared with thermally removable nanoparticle templates: an efficient electrocatalyst for oxygen reduction reaction, J. Am. Chem. Soc. 137 (2015) 5555–5562.

[50] K. Liu, S. Kattel, V. Mao, G. Wang, Electrochemical and computational study of oxygen reduction reaction on nonprecious transition metal/nitrogen doped carbon nanofibers in acid medium, J. Phys. Chem. C 120 (2016) 1586–1596.

[51] Y. Dai, Y. Chan, B. Jiang, L. Wang, J. Zou, K. Pan, H. Fu, Bifunctional Ag/Fe/N/C catalysts for enhancing oxygen reduction via cathodic biofilm inhibition in microbial fuel cells, ACS Appl. Mater. Interfaces 8 (2016) 6992–7002.

[52] B.S. Yeo, A.T. Bell, Enhanced activity of gold-supported cobalt oxide for the electrochemical evolution of oxygen, J. Am. Chem. Soc. 133 (2011) 5587–5593.

[53] M.-R. Gao, S. Liu, J. Jiang, C.-H. Cui, W.-T. Yao, S.-H. Yu, In situ controllable synthesis of magnetite nanocrystals/$CoSe_2$ hybrid nanobelts and their enhanced catalytic performance, J. Mater. Chem. 20 (2010) 9355–9361.